Indian J. pure appl. Math., **27**(11) : 1137-1150, November 1996

ON THE DISTRIBUTIONS OF AXIAL VELOCITY AND PRESSURE GRADIENT IN A PULSATILE FLOW OF BLOOD THROUGH A CONSTRICTED ARTERY

H. P. MAZUMDAR[1], U. N. GANGULY (HABISHYASI)[2], S. GHORAI[3] AND D. C. DALAL[1]

[1]*Indian Statistical Institute, Calcutta* 700 035
[2]*Bonhooghly College of Commerce, Calcutta* 700 035
[3]*Department of Mathematics, University of Leeds, U.K.*

(*Received* 9 *August* 1995; *after revision* 29 *February* 1996; *accepted* 9 *April* 1996)

The present paper deals with the time variations of some characteristics of the Newtonian flow of blood through a stenosed artery. Considering the arterial vessel to be a circular cylindrical tube, the non-uniform suspension viscosity of blood to obey an approximate model and prescribing a volume flux, series solutions are obtained for the distributions of axial velocity and pressure gradient. Effects of the Womersley parameter and a parameter depicting the hematocrit distribution in the blood on these characteristics of the flow field are discussed.

1. INTRODUCTION

The study of the time variation of various characteristics of viscous incompressible fluid flows through cylindrical tubes is quite relevant to the construction of more realistic models for blood flows through arteries and veins. Young[1] presented an excellent analysis of flow through an occluded tube under a pulsatile pressure gradient. After the publication of Young's poineering work, investigations were carried out by authors e.g., Forrester and Young[2], Young and Tsai[3], Back *et al.*[4] on various aspects of blood flow through partially occluded tube. Ahmed and Giddens[5] and Ojha *et al.*[6] considered sophisticated measurements using, repectively Laser Doppler Anemometry (LDA) and Photocromic Tracer Method to study mainly the changes in pulsatile flow velocity profiles through consrticted tubes. Construction of mathematical-numerical models, incorporating hydrodynamical aspects, for blood flow in stenosed artery also received much attention. Lee and Fung[7] obtained solution to the steady axisymmetric flow of a viscous incompressible fluid through a locally constricted circular cylindrical tube at low Reynolds numbers by conformal mapping technique. The numerical results presented by them for the streamlines and distributions of velocity, pressure, vorticity, and shear stress were

used for analysing the blood flow in a circular cylindrical tube with a local constriction. Ling and Atabek[8] carried out nonlinear analysis of pulsatile flow in arteries. They presented an approximate numerical method for calculating flow profiles in arteries. The computed theoretical results on the velocity distribution and wall shear at a given location in terms of pressure, pressure gradient and pressure-radius relation agreed well with the corresponding measured data. As relevant to velocity profiles within the arterial system, Blick and Stein[9] derived simple solution for pulsatile flow in rigid tubes by applying variational method. Rao[10] presented a complete and correct solution for the unsteady flow in an uniform elliptical pipe in terms of Mathieu functions. Rao and Padmavathi[11] investigated the pulsatile flow of an incompressible viscous fluid also in an elliptical pipe but of slowly varying cross-section. They obtained asymptotic series solutions for the velocity distribution and pressure gradient in terms of Mathieu functions for a low Reynolds number flow in which the volume flux is prescribed.

In this paper, we investigate the axial velocity distributions and the pressure gradients of the Newtonian flow of blood through a constricted circular cylindrical arterial tube for various values of hematocrit and the Womersley parameter.

2. Shape of the Constriction

Blood, may approximately be treated as a Newtonian fluid when flowing through large arteries (Rodkiewicz[12]). Again, large arteries are prone to atherosclerotic development (Padmanabhan[13]). Several models have been proposed to define the geometry of the constriction. Most commonly used shape of the constriction is represented by a cosine curve e.g.,

$$R^*(z^*) = a - \delta\left(1 + \cos\frac{\pi z^*}{2z_0}\right) \text{ for } -2z_0 \le z^* \le 2z_0 \qquad \ldots (1)$$

$$= a \text{ otherwise}$$

where a is the radius of the arterial tube outside the stenotic region, $4z_0$ the length of stenois and 2δ the maximum height of the stenosis. The form (1) was originally suggested by Young[1]. Lee and Fung[14] specified the geometry of the constriction as a bell-shaped curve while Schneck and Ostrach[15] modelled the stenosed artery by a channel having a small exponential divergence. The geometry of the bell-shaped curve of Lee and Fung[14] is, given by

$$\frac{R^*(z^*)}{a} = 1 - b\exp\left(-\frac{cz^{*2}}{a^2}\right) \qquad \ldots (2)$$

where a is the radius of the tube far away from the origin, b the amplitude of the local constriction ($b > 0$), and c the sharpness factor. It is to be mentioned that the role of the stars, as in (1), (2) and throughout the analysis is to denote dimensional variables, such that when these same variables are written without stars they are dimensionless.

In the present analysis, we consider the form (2) for the shape of the constriction with choices of b and c, respectively as 0.25 and 1.

3. Model for Viscosity

It is known that blood is a complex fluid with formed elements (red cells, white cells and platelets) suspended in plasma. The percent volume concentration of red cells in the whole blood is called the hematocrit. For an adult it is approximately 40-45% (Oka[17]). Viscosity of blood, and thus the velocity distribution depend on the concentration of cells. Lih[17] postulated a model for the nonuniform suspension viscosity for blood, flowing through an arterial tube of uniform cross section e.g.,

$$\mu^*(r^*) = \mu_0^* \{1 + k[1 - (r^*/a)^n]\} \quad \ldots (3)$$

where $k = Bh_m$, B is a constant having the value 2.5 and h_m the maximum hematocrit at the centre. μ_0^*, the viscosity of the plasma is assumed constant. n is a parameter determining the shape of the cell distribution in blood flow. In the present analysis, we shall consider the case $n = 2$ for which the shape of the profile is parabolic. Formula (3) indicates that viscosity increases as we move from the wall towards the centre where it is maximum. Also, it may be imagined that near the wall there is a thin layer dominated by plasma. In the cases of axisymmetric mild constrictions represented by (1) and (2), as we move from the beginning of the stenosis along the wall, it is expected that the plasma layer will be thinner and thinner till we reach the peak of the stenosis where it is thinnest. Recently, Haldar and Andersson[18] have shown that the plasma layer thickness varies along the length of the tube of stenosis and attains its minimum value at the throat of the stenosis. Presumably, changes in viscosity by little amounts along the stenosis are not out of question. It appears that the model (3) for nonuniform viscosity can cope with this situation. Further, we shall be concerned here with the case of mild stenosis [the form (2) with $b = 0.25$, $c = 1$] and as possibly there may occur no serious error, we shall apply also the model (3) for viscosity to characterise the flow in the stenotic region.

4. Basic Equations

When there is no variation of viscosity μ^*, the unsteady, axisymmetric incompressible Newtonian fluid flow through the region $0 \le r^* \le a$, $0 \le \theta \le 2\pi$, $-\infty < z^* < \infty$ of a circular cylindrical tube is governed by the equations

$$\rho^*\left(\frac{\partial v_r^*}{\partial t^*} + v_r^*\frac{\partial v_r^*}{\partial r^*} + v_z^*\frac{\partial v_r^*}{\partial z^*}\right) = -\frac{\partial p^*}{\partial r^*} + \mu^*\left(\frac{\partial^2 v_r^*}{\partial r^{*2}} + \frac{1}{r^*}\frac{\partial v_r^*}{\partial r^*} + \frac{\partial^2 v_r^*}{\partial z^{*2}} - \frac{v_r^*}{r^{*2}}\right) \quad \ldots (4)$$

$$\rho^*\left(\frac{\partial v_z^*}{\partial t^*} + v_r^*\frac{\partial v_z^*}{\partial r^*} + v_z^*\frac{\partial v_z^*}{\partial z^*}\right) = -\frac{\partial p^*}{\partial z^*} + \mu^*\left(\frac{\partial^2 v_z^*}{\partial r^{*2}} + \frac{1}{r^*}\frac{\partial v_z^*}{\partial r^*} + \frac{\partial^2 v_z^*}{\partial z^{*2}}\right) \quad \ldots (5)$$

where v_r^* is the radial velocity, v_z^* the axial velocity, p^* the pressure and ρ^* the constant density. The equation of continuity is given by

$$\frac{\partial v_r^*}{\partial r^*} + \frac{v_r^*}{r} + \frac{\partial v_z^*}{\partial z^*} = 0. \qquad \ldots (6)$$

On the inner wall of the tube $r^* = a$ and $r^* = R^*(z^*)$ the no-slip condition requires that

$$v_r^* = v_z^* = 0 \quad \text{at} \quad r^* = a \text{ and } r^* = R^*(z^*).$$

If variation of viscosity be taken into account according to the formula (3), eqns. (4) and (5) are to be replaced by

$$\rho^* \left(\frac{\partial v_r^*}{\partial t^*} + v_r^* \frac{\partial v_r^*}{\partial r^*} + v_z^* \frac{\partial v_r^*}{\partial z^*} \right) = -\frac{\partial p^*}{\partial r^*} + 2\mu_0^* \frac{\partial v_r^*}{\partial r^*} \cdot \frac{\partial \otimes}{\partial r^*} + \mu_0^* \otimes \left[\frac{\partial^2 v_r^*}{\partial r^{*2}} + \frac{1}{r^*} \frac{\partial v_r^*}{\partial r^*} + \frac{\partial^2 v_r^*}{\partial z^{*2}} - \frac{v_r^*}{r^{*2}} \right] \qquad \ldots (7)$$

$$\rho^* \left(\frac{\partial v_z^*}{\partial t^*} + v_r^* \frac{\partial v_z^*}{\partial r^*} + v_z^* \frac{\partial v_z^*}{\partial z^*} \right) = -\frac{\partial p^*}{\partial z^*} + \mu_0^* \frac{\partial \otimes}{\partial r^*} \left(\frac{\partial v_r^*}{\partial z^*} + \frac{\partial v_z^*}{\partial r^*} \right) + \mu_0^* \otimes \left(\frac{\partial^2 v_z^*}{\partial r^{*2}} + \frac{1}{r^*} \frac{\partial v_z^*}{\partial r^*} + \frac{\partial^2 v_z^*}{\partial z^{*2}} \right) \qquad \ldots (8)$$

where $\otimes = 1 + k\left(1 - \frac{r^{*2}}{a}\right)$.

We shall consider $\varepsilon = \frac{a}{L}$, where L is the characteristic length of the tube, as a perturbation parameter. We introduce the nondimensional quantities as follows :

$$\left.\begin{aligned} & r = \frac{r^*}{a};\ z = \frac{z^*}{L},\ p = \frac{p^*}{\rho^* U_0^{*2}/\mathrm{Re}\,\varepsilon},\ t = \bar{\omega}\, t^* \\ & Re = \frac{U_0^* a}{\nu^*},\ \bar{\omega} = \frac{\alpha^2 \nu^*}{a^2},\ \nu^* = \frac{\mu^*}{\rho^*} \\ \text{and} \quad & (\varepsilon v_r, v_z) = \left(\frac{v_r^*}{U_0^*}, \frac{v_z^*}{U_0^*} \right) \end{aligned}\right] \qquad \ldots (9)$$

where ρ^* is the density of the fluid, U_0^* the characteristic velocity, $\bar{\omega}$ the frequency of the pulsatile flow, Re the Reynolds number and α the well known Womersley parameter.

In view of the relations (9), eqns. (7), (8) and the continuity relation (6) are expressible in terms of nondimensional quantities as

$$\alpha^2 \frac{\partial v_r}{\partial t} + \varepsilon\, Re\, \Delta_1 v_r = -\frac{1}{\varepsilon^2} \frac{\partial p}{\partial r} + \otimes \left[\Delta_2 v_r - \frac{v_r}{r^2} \right] + 2 \frac{d\otimes}{dr} \cdot \frac{\partial v_r}{\partial r} \qquad \ldots (10)$$

$$\alpha^2 \frac{\partial v_z}{\partial t} + \varepsilon\, Re\, \Delta_1 v_z = -\frac{\partial p}{\partial z} + \otimes (\Delta_2 v_z) + \frac{d\otimes}{dr}\left\{ \varepsilon^2 \cdot \frac{\partial v_r}{\partial z} + \frac{\partial v_z}{\partial r} \right\} \quad \ldots (11)$$

$$\frac{\partial v_r}{\partial r} + \frac{v_r}{r} + \frac{\partial v_z}{\partial z} = 0 \quad \ldots (12)$$

where $\Delta_1 = v_r \frac{\partial}{\partial r} + v_z \frac{\partial}{\partial z}$, $\Delta_2 = \frac{\partial^2}{\partial r^2} + \frac{1}{r}\frac{\partial}{\partial r} + \varepsilon^2 \frac{\partial^2}{\partial z^2}$.

The boundary conditions are now read as

$$(v_r, v_z) = 0 \quad \text{at} \quad r = R(z),\ R(z) = \frac{R^*(z^*)}{a}. \quad \ldots (13)$$

The nondimensional flux across any cross-section is prescribed by

$$\int_0^{R(z)} v_z\, r\, dr = \pi(1 + e^{it}). \quad \ldots (14)$$

5. Axial Velocity : Pressure Gradient

Let us assume a solution in the form

$$(v_r, v_z, p) = \sum_0^\infty \varepsilon^m (v_{rm}, v_{zm}, p_m) \quad \ldots (15)$$

Substituting (15) in eqns. (10)-(12), we obtain (remembering that p_0, p_1 etc. are independent of r) equating like powers of ε

$$\alpha^2 \frac{\partial v_{r0}}{\partial t} = -\frac{dp_2}{dr} + \otimes \left[\frac{\partial^2 v_{r0}}{\partial r^2} + \frac{1}{r}\frac{\partial v_{r0}}{\partial r} - \frac{v_{r0}}{r^2} \right] + 2\frac{d\otimes}{dr} \cdot \frac{\partial v_{r0}}{\partial r} \quad \ldots (16)$$

$$\alpha^2 \frac{\partial v_{z0}}{\partial t} = -\frac{dp_0}{dz} + \otimes \left[\frac{\partial^2 v_{z0}}{\partial r^2} + \frac{1}{r}\frac{\partial v_{z0}}{\partial r} \right] + \frac{d\otimes}{dr} \cdot \frac{\partial v_{z0}}{\partial r} \quad \ldots (17)$$

$$\frac{\partial v_{r0}}{\partial r} + \frac{v_{r0}}{r} + \frac{\partial v_{z0}}{\partial z} = 0 \quad \ldots (18)$$

$$\alpha^2 \frac{\partial v_{z1}}{\partial t} + \mathrm{Re}\, \Delta_{10} v_{z0} = -\frac{dp_1}{dz} + \left[\frac{\partial^2 v_{z1}}{\partial r^2} + \frac{1}{r}\frac{\partial v_{z1}}{\partial r} \right] + \frac{d\otimes}{dr} \cdot \frac{\partial v_{z1}}{\partial r} \quad \ldots (19)$$

etc.

where $\Delta_{10} = v_{r0}\frac{\partial}{\partial r} + v_{z0}\frac{\partial}{\partial z}$.

We attempt here to determine the zeroth order solution for the axial velocity and the corresponding pressure gradient. This is analogous to the treatment of one

dimensional model for blood flow through the artery under pulsatile pressure gradient. Modification of the flow field due to assumed dependence of viscosity on the distribution of red cells would be of high interest in this work.

For this purpose, we write

$$v_{z0} = v_{z0s} + v_{z0T}\, e^{it}, \quad \frac{dp_0}{dz} = p_{0s} + p_{0T}\, e^{it}. \qquad \ldots (20)$$

Substituting (20) in (17) and comparing the coefficient of e^{int}, $n = 0, 1$ we obtain

$$\otimes\left[\frac{\partial^2}{\partial r^2} v_{z0s} + \frac{1}{r}\frac{\partial}{\partial r} v_{z0s}\right] - 2kr\frac{\partial v_{z0s}}{\partial r} - p_{0s} = 0 \qquad \ldots (21)$$

$$\otimes\left[\frac{\partial^2}{\partial r^2} v_{z0T} + \frac{1}{r}\frac{\partial}{\partial r} v_{z0T}\right] - 2kr\frac{\partial v_{z0T}}{\partial r} - p_{0T} - \alpha_1^2 v_{z0T} = 0 \qquad \ldots (22)$$

where $\alpha_1^2 = i\alpha^2$.

The boundary condition $v_z = 0$ at $r = R(z)$ is now read as

$$v_{z0s} = 0, \; v_{z0T} = 0 \text{ at } r = R(z). \qquad \ldots (23)$$

Relation (14) can now be expressed as

$$\int_0^{R(z)} v_{z0s}\, r\, dr = \pi, \quad \int_0^{R(z)} v_{z0T}\, r\, dr = \pi. \qquad \ldots (24)$$

Solution of (21) with the conditions that velocity should not be infinite on the tube axis and $v_{z0s} = 0$ at $r = R(z)$, is obtained easily as

$$v_{z0s} = \frac{p_{0s}}{4k}\left[\log\{1 + k[1 - R(z)^2]\} - \log\{1 + k(1 - r^2)\}\right]. \qquad \ldots (25)$$

In order to solve eqn. (22), we put

$$v^+_{z0T} = v_{z0T} + \frac{p_{0T}}{\alpha_1^2}. \qquad \ldots (26)$$

In view of the relation (26), eqn. (22) reduces to

$$\left[\frac{\partial^2}{\partial r^2} v^+_{z0T} + \frac{1}{r}\frac{\partial}{\partial r} v^+_{z0T}\right] - 2kr\frac{\partial}{\partial r} v^+_{z0T} - \alpha_1^2 v^+_{z0T} = 0. \qquad \ldots (27)$$

We seek solution of (27) in the form

$$v^+_{z0T} = \sum c_\beta\, r^\beta. \qquad \ldots (28)$$

Substituting (28) in (27), we obtain after some calculations

$$c_\beta = \frac{\beta(\beta-2)\,k+\alpha_1^2}{(1+k)\,\beta^2}\,c_{\beta-2},\ \beta \geq 2 \qquad \ldots (29)$$

and $$c_1 = c_3 = c_5 = \ldots = 0. \qquad \ldots (30)$$

Taking the relations (28)-(30) into account in (26), we obtain

$$v_{z0T} = \frac{p_{0T}}{\alpha_1^2}\left[\frac{1+\frac{c_2}{c_0}r^2+\frac{c_4}{c_0}r^4+\ldots}{1+\frac{c_2}{c_0}R(z)^2+\frac{c_4}{c_0}R(z)^4+\ldots}-1\right]. \qquad \ldots (31)$$

Substituting (25) into the first relation of (24), we obtain after effecting integration

$$p_{0s} = \frac{4k\pi}{\frac{R(z)^2}{2}+\frac{(1+k)}{2k}\left[\log\left|1+k-kR(z)^2\right|-\log(1+k)\right]}. \qquad \ldots (32)$$

Substituting (31) into the second relation of (24), we obtain after some calculations

$$p_{0T} = \frac{\pi\alpha_1^2}{S} \qquad \ldots (33)$$

where

$$S = \frac{\frac{R(z)^2}{2}+\frac{c_2}{c_0}\frac{R(z)^4}{4}+\frac{c_4}{c_0}\cdot\frac{c_2}{c_0}\frac{R(z)^6}{6}+\ldots.}{1+\frac{c_2}{c_0}R(z)^2+\frac{c_4}{c_0}\cdot\frac{c_2}{c_0}\cdot R(z)^4+\ldots}. \qquad \ldots (34)$$

From (25), (31), (32), (33) and (34), we calculate $v_{z0s}+\mathcal{R}(v_{z0T}\,e^{it})$ and $p_{0s}+\mathcal{R}(p_{0T}\,e^{it})$ for different values of the hematocrit parameter k and the Womersley parameter α. $\mathcal{R}(\ )$ stands for the real part of the quantity in the parenthesis.

6. Discussions of Results

The shape of the constriction considered for numerical computation, is described by $R(z) = R^*(z^*)/a = 1 - 0.25e^{-z^2}$. Clearly $z = 0$ is the point of maximum constriction. Also the constriction is symmetric about $z = 0$. We compute the axial velocity v_{z0} and the pressure gradient dp_0/dz at different times with various choices of the Womersley parameter α and the hematocrit parameter k. The results are presented graphically. In Fig. 1, dp_0/dz is plotted against z at $t = 0$ for different values of α e.g., $\alpha = 0.5, 2, 4$. The value of k being chosen as 0.25. It is clear that magnitude of the pressure gradient attains maximum at the point of maximum constiction. In Fig. 2, dp_0/dz is plotted against z at $t = 2.5$ for different choices of k,-e.g., $k = 0.25, 0.50, 0.75, 1$. α being chosen equal to 4. The pressure gradient is found to decrease with the increase of k.

In Figs. 3, 4 and 5, the pressure gradient curves for different values of t are shown, respectively for the cases (i) $\alpha = 2$, $k = 0.25$, (ii) $\alpha = 2$, $k = 0.75$ (iii) $\alpha = 3$, $k = 0.50$. Careful observation indicates that the curve for $t = 2.5$ of case (ii) has got more than one extremum point. In Fig. 6, the axial velocity v_{z0} is plotted against r for values of t e.g., $t = 0$, 0.5, 1, 1.5, 2, 2.5 at the throat $z = 0$. The values of α and k are being chosen, respectively as 2 and 0.25. It is noticable that z_{z0} decreases at any $r(< 0.75)$ as t advances. v_{z0} is maximum for all t at the point of maximum constriction and decreases with the increases of r. All the curves merge at $r = 0.75$ where v_{z0} assumes zero value. Variations of v_{z0} with time, at the throat $z = 0$ are also demonstrated for two other cases e.g., (i) $\alpha = 3$, $k = 0.25$ (ii) $\alpha = 4$, $k = 0.25$. (Figs. 7 and 8). Qualitative features remain similar to the case of Fig. 6.

We plot v_{z0} at $t = 2.5$ and at the throat $z = 0$ for values of $\alpha = 2$, 3, 4 in the same Fig. 9. The value of k being chosen as same 0.25. It is clear that in the core region v_{z0} increases with the increase of α. The curves cross in between $r = 0.4$ and $r = 0.45$. Opposite feature is noticed after the cross over until all the curves merge at $r = 0.75$.

In Fig. 10, the variations of v_{z0} at $t = 2.5$ and at the throat $z = 0$ are shown for values of k e.g., $k = 0.25$, 0.5, 1. The value of α is chosen as 2. In the core region v_{z0} is found to decrease with the increase of k. The curves cross at about $r = 0.45$. Opposite feature occurs after the cross over also in this case until all the curves merge at $r = 0.75$.

7. Concluding Remarks

It is implied with the zeroth approximation that the nonlinear terms are not important and the radial pressure gradient is negligible. Such simplifications may however, be justified for the low Reynolds number flow and when the cross-section of the tube varies slowly (MacDonald[9]). Even under this simplified situation both Womersley parameter α and the hematocrit parameter $k(= Bh_m)$ have been found to influence the pulsatile Newtonian flow of blood through the circular cylindrical arterial tube significantly. α^2 is known to be the ratio of the viscous diffusion time to the period of oscillation, or an unsteady Reynolds number (Berger[20]). In the human arterial system, α takes numerical values between 1 and 4 (Padmanavan[13]). In the present analysis, we have used values upto 4 for α. During the flow, the amount of internal friction is enhanced due to presence of red cells in plasma. Hence, hematocrit is a major variable of blood viscosity. Under pathologic condition hematocrit may vary from about 0.3 to 0.7 (Quemada[21]). We have considered here low and moderate values for the maximum hematocrit h_m.

The present investigation warrants higher order calculations and evaluations of both axial and cross velocity components and as well as other physiologically important factors, e.g., shear stress on the boundary and impedence to gain more insight into the problem. The authors plan to carry out such calculations and report the results in a future paper.

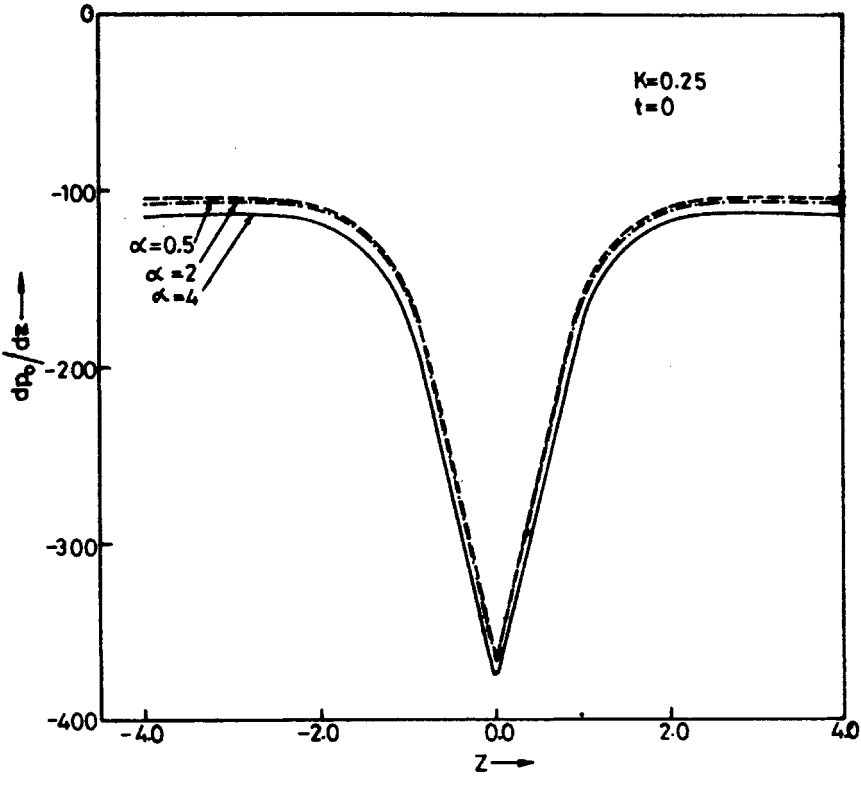

FIG. 1. Plot of dp_0/dz vs. z for values of α = 0.5, 2, 4 (t = 0, k = 0.25).

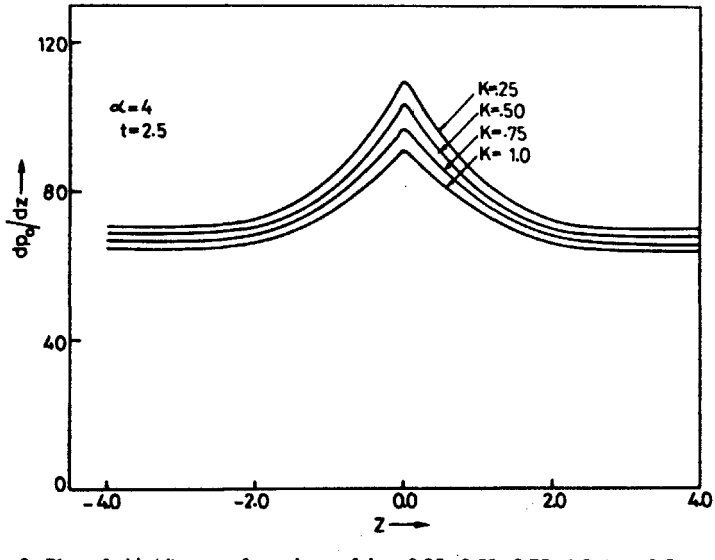

FIG. 2. Plot of dp_0/dz vs. z for values of k = 0.25, 0.50, 0.75, 1.0 (t = 2.5, α = 4).

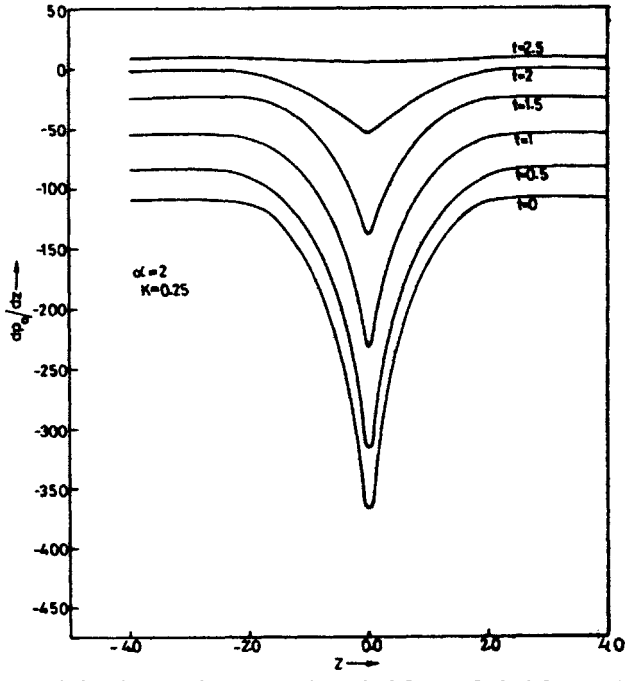

FIG. 3. Plot of dp_0/dz vs. z for values of t = 0, 0.5, 1, 1.5, 2, 2.5 (α = 2, k = 0.25).

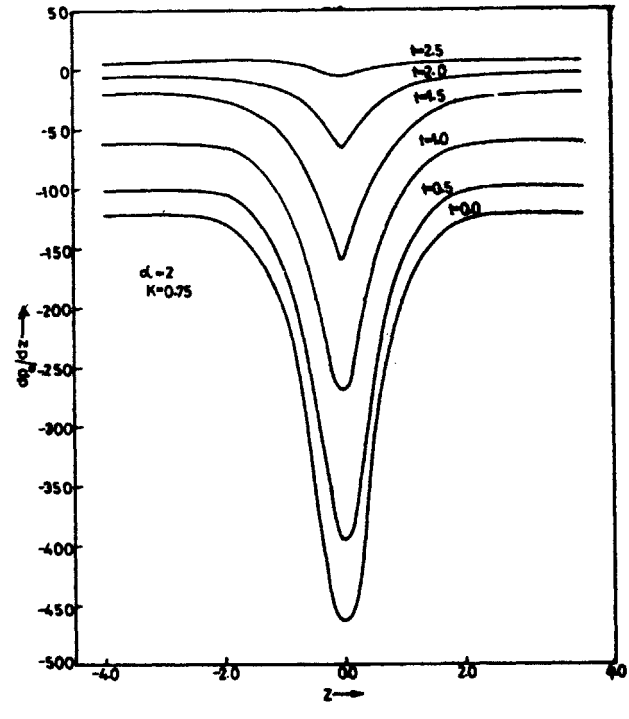

FIG. 4. Plot of dp_0/dz vs. z for values of t = 0, 0.5, 1, 1.5, 2, 2.5 (α = 2, k = 0.75).

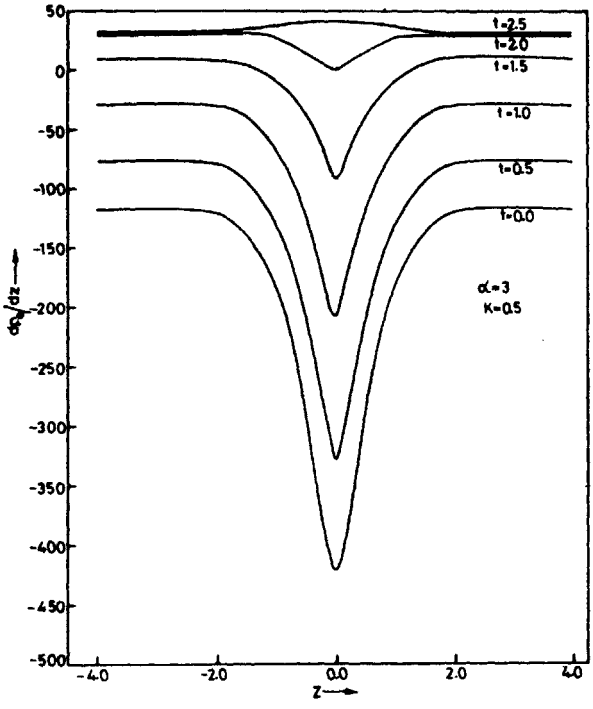

FIG. 5. Plot of dp_0/dz vs. z for values of t = 0, 0.5, 1, 1.5, 2, 2.5 (α = 3, k = 0.5).

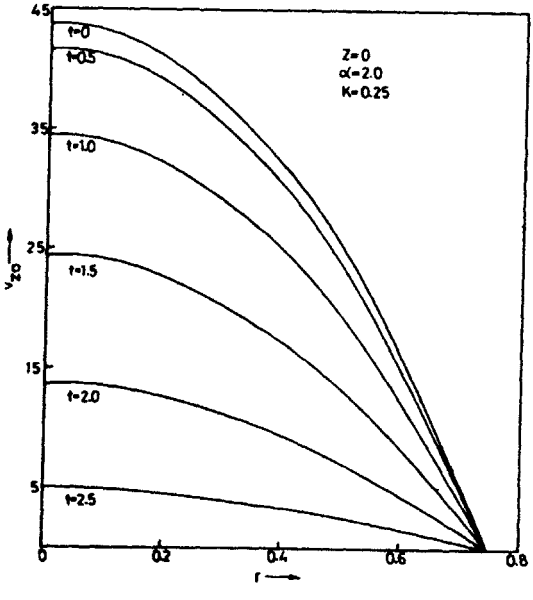

FIG. 6. Plot of v_{z0} vs. r for values of t = 0, 0.5, 1, 1.5, 2, 2.5 (z = 0, α = 2, k = 0.25).

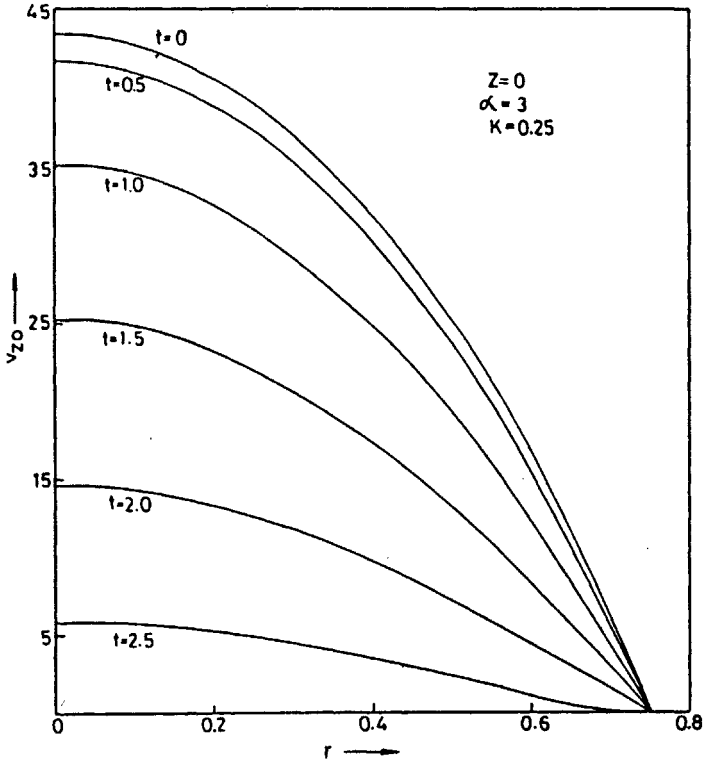

FIG. 7. Plot of v_{z0} vs. r for values of t = 0, 0.5, 1, 1.5, 2, 2.5 (z = 0, α = 3, k = 0.25).

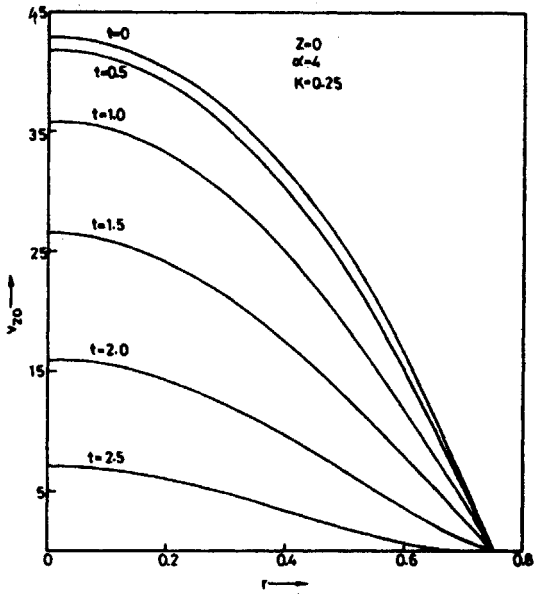

FIG. 8. Plot of v_{z0} vs. r for values of t = 0, 0.5, 1, 1.5, 2, 2.5 (z = 0, α = 4, k = 0.25).

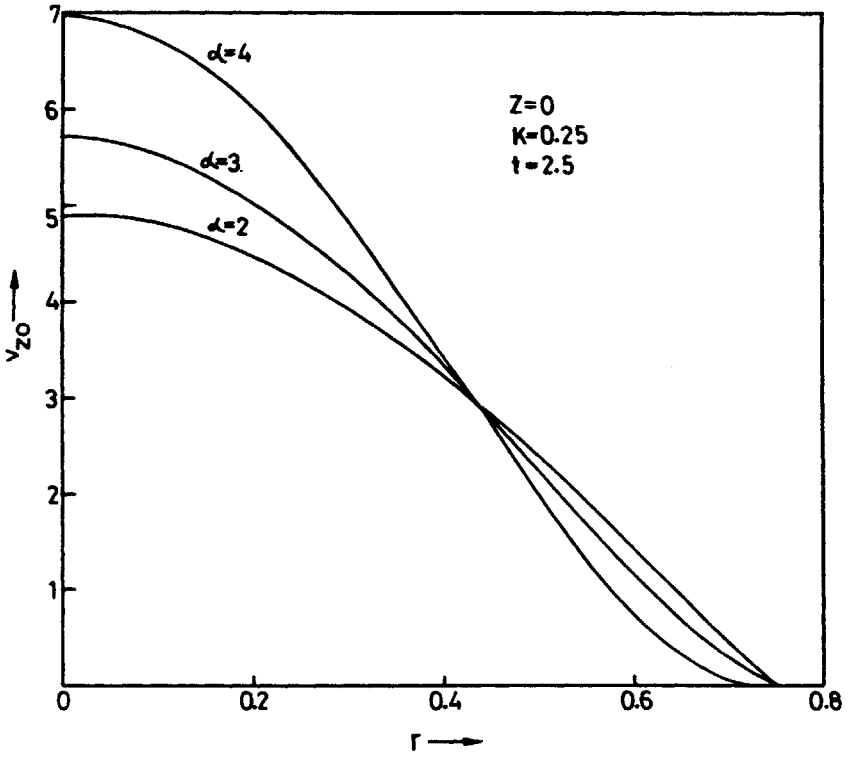

FIG. 9. Plot of v_{z0} vs. r for values of α = 2, 3, 4 (z = 0, k = 0.25, t = 2.5).

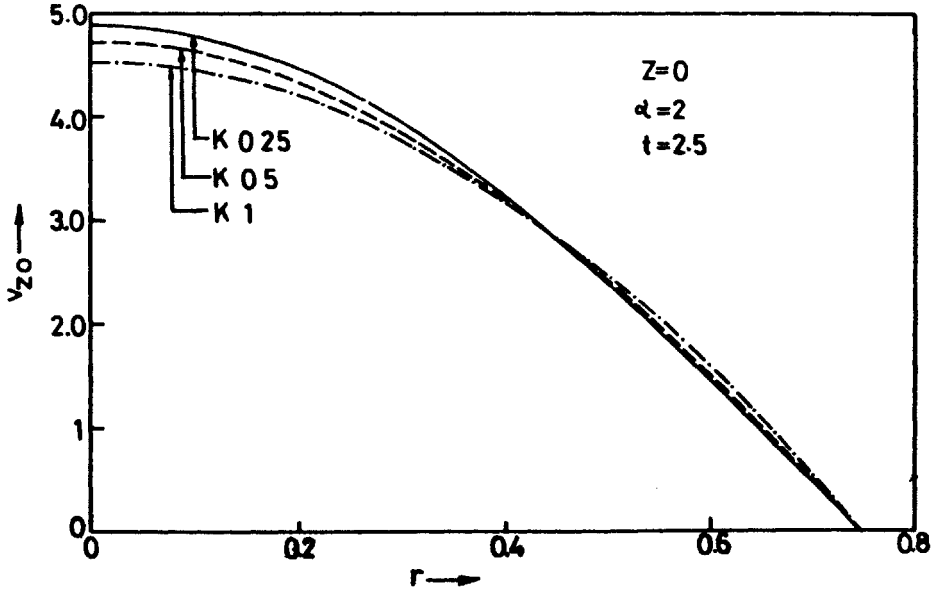

FIG. 10. Plot of v_{z0} vs. r for values of k = 0.25, 0.5, 1 (z = 0, α = 2, t = 2.5).

ACKNOWLEDGEMENT

We express our deep gratitude to the referee for his valuable suggestions in the improvement of the paper.

REFERENCES

1. D. F. Young, *J. Engng. for Industry, Trans. ASME* **90** (1968), 248-54.
2. J. H. Forrester and D. F. Young, *J. Biomech.* **3** (1970), 297-305, 307-16.
3. D. F. Young and F. Y. Tsai, *J. Biomech.* **6** (1973), 395, 547.
4. L. D. Back *et al.*, *J. Biomech.* **10** (1977), 339-53.
5. S. Ahmed and D. P. Giddens, *J. Biomech.* **17** (1984), 695-705.
6. M. Ojha *et al.*, *J. Fluid Mech.* **203** (1989), 173-97.
7. J. S. Lee and Y. C. Fung, *J. Appl. Mech.* **37** (1970), 9-16.
8. S. C. Ling and H. B. Atabek, *J. Fluid Mech.* **55** (1972), 493.
9. L. F. Blick and P. D. Stein, *J. Biomech. Engng.* (1984).
10. A. Ramachandra Rao, *J. Indian Inst. Sci.* **66** (1986), 543-45.
11. A. Ramachandra Rao and K. Padmavathi, *Int. J. Non-linear Mech.* **28** (1993), 455-66.
12. C. M. Rodkiewicz, in : *Arteries and Arterial Blood Flow* (ed. C. M. Rodkiewicz), Springer-Verlag, Wien, 1983, pp. 327-411.
13. N. Padmanabhan, *Med. Biol. Engngs. & Comput.* **18** (1980), 281-86.
14. J. S. Lee and Y. C. Fung, *Microvasc. Res.* **3** (1971), 272.
15. D. J. Schneck and S. Ostrach, *J. Fluid Engng. Trans. ASME.* **16** (1975), 353-60.
16. S. Oka, *Cardiovascular Hemorheology*, Cambridge University Press, Cambridge, London, 1981, p. 28.
17. M. M. Lih, *Transport Phenomena in Medicine and Biology*. John Wiley New York, 1975, pp. 378-414.
18. K. Haldar and H. I. Andersson, Two-layered model of blood flow through stenosed arteries, *Acta Mechanica*, to appear (1995).
19. D. A. MacDonald, *J. Biomechanics.* **12** (1979), 13-20.
20. S. A. Berger, *Am. Math. Soc.* **141** (1993), 479-511.
21. D. Quemada, in : *Arteries and Arterial Blood Flow* (ed. C. M. Rodkiewicz), Springer-Verlag, Wien, 1983, pp. 1-127.